RERTR 2016 – 37TH INTERNATIONAL MEETING ON
REDUCED ENRICHMENT FOR RESEARCH AND TEST REACTORS

OCTOBER 23-27, 2016
RADISSON BLU ASTRID HOTEL
ANTWERP, BELGIUM

Quantitative comparability of heavy ion and in-pile induced IDL growth in UMo/Al fuels

H. Breitkreutz, J. Hingerl, A. Heldmann, Ch. Steyer, T. Zweifel, R. Jungwirth, J. Shi, W. Petry
Forschungs-Neutronenquelle Heinz Maier-Leibnitz (FRM II)
Technische Universität München, Lichtenbergstr. 1, 85747 Garching, Germany

ABSTRACT

Irradiation with heavy ions is an increasingly often used tool to quickly reproduce and simulate certain effects of in-pile irradiation tests. Based on a SRIM/TRIM dataset for the deposition of energy and the creation of vacancies in UMo/Al fuels by in-pile fission products as well as out-of-pile Iodine-127 ions (80 MeV), a formula for the conversion of ion flux and fluency in the corresponding fission rate and burn-up equivalents has been derived.

A comparison of thicknesses and growth dynamics of out-of-pile produced interdiffusion layers with predictions based on in-pile data demonstrates the applicability of the presented approach as well as the reliability of heavy ion irradiations. The data from two I-127 irradiation experiments thereby supports the current understanding of the Arrhenius-like in-pile IDL growth, i.e. its dependency on fission rate / ion flux, irradiation time and temperature.

1. Introduction

During in-pile irradiation of UMo/Al based fuels, diffusion occurs between the UMo and the Al matrix [1]. Thereby, an amorphous U-Al interdiffusion layer (IDL) at the interface between the UMo and the Al is formed which has been identified as the main cause for unacceptable fuel plate swelling at low burn-up [2, 3, 4, 5, 6, 7, 37]. Besides purely thermal effects, one of the driving forces for this diffusion process is the recoil of the fission products generated during irradiation in combination with elevated temperatures [8]. Even though in the meantime measures have been taken to mitigate the IDL growth by means of diffusion barriers [9, 10, 11] and Si addition to the matrix [12, 13, 14, 15], it is still necessary to understand the development of the IDL, which seems to reappear at high burn-up even in coated fuels.

Heavy ion irradiation with Iodine-127 at 80MeV has been frequently used as a tool to quickly reproduce such a diffusion layer in UMo/Al based samples [16, 17, 18, 11, 19, 20]. The main advantages of heavy ion irradiation compared to in-pile irradiation are time, simplified handling and cost savings: A diffusion layer similar to weeks of in-pile irradiation can be obtained within a

day of heavy ion irradiation. Furthermore, because the incident energy of the ions is below the Coulomb barrier, no additional radioactivity is created in the sample.

This paper first establishes a quantitative comparison between heavy ion and in-pile irradiated material, i.e. between ion flux and fluency and the respective in-pile equivalents, fission rate and fission density / burn-up.

For this, the energy deposition for fission products in a simple UMo/Al layer system (Fig. 1a) is simulated using SRIM/TRIM and compared to that of Iodine-127 ions with 80MeV that are penetrating a thin layer of UMo (thickness $d_{\mathrm{ion}}^{\mathrm{U}}$, Fig. 1b) on top of an Aluminium substrate (entitled U8Mo/Al) or the respective inverse system with an Al-layer (thickness $d_{\mathrm{ion}}^{\mathrm{Al}}$) on top of a Uranium substrate (entitled Al/U10Mo). The thickness of the top layer can be varied and is controlled through the manufacturing process (here: physical vapor deposition, PVD).

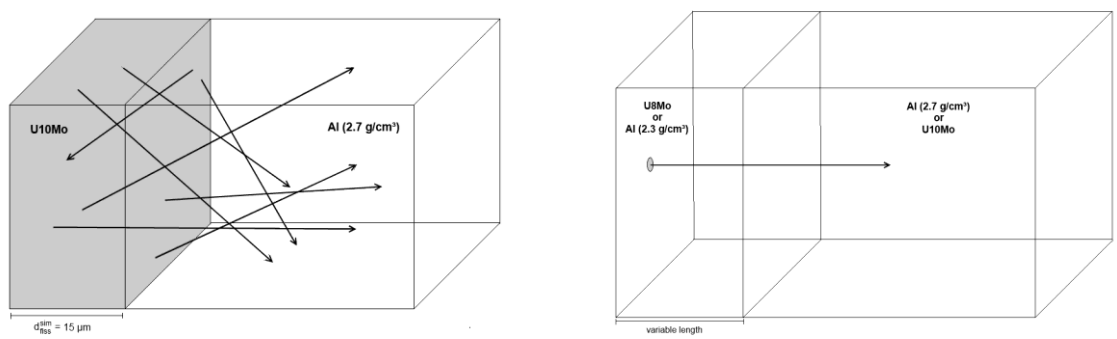

Figure 1: Left: Simulated sample for the fission fragments. The fission fragments were generated in the shaded area starting in random directions. Right: Simulated sample for heavy ions. The ions in the simulation were generated in a point source, starting straight into the sample.

To a large extent, the results for the monolithic UMo/Al systems regarded here are also applicable to dispersion fuel of the same constituents, as the diameter of the UMo particles is generally large compared to the range R_0 of fission products and ions; Kim [26] discusses curvature effects, touching particles and overlapping IDLs.

2. Simulations

The simulations were performed using James Ziegler's SRIM/TRIM [27]. The option "Detailed Calculation with Full Damage Cascades" was used to include the maximum detail in the simulations [33]. All calculations were performed for U 8wt.% Mo (U8Mo) for the fission fragments and UMo/Al layer systems; U 10wt.% Mo (U10Mo) was used for Al/UMo layer systems. For the latter, an Aluminium density of only 2.3 g/cm³ was used, as this was the density determined by Hingerl [30] for layers that were deposited on a U10Mo substrate using PVD. Otherwise, the density of the Aluminium was 2.7 g/cm³. The two different UMo alloys were used for technical reasons.

Fission fragments were simulated as discussed in detail by Heldmann [29] with an improved sampling algorithm. To limit the number of simulations, the fragments were weighted and combined into representative fragments. The weight is constructed from two factors, the probability of production, which is varying through several orders of magnitude; and from the energy loss due to ionization as this is the major energy loss mechanism. Accordingly, the fission

fragments were combined into 47 virtual "representative fission fragments" with a fixed atomic number, weighted masses and averaged creation probabilities.

In order to calculate the total energy deposition and lattice damage distribution, the single damage distributions of the fission fragments were summed up by weighting their respective damage distributions with their probability of creation. The result, units [eV / FF Å] for energy deposition and [1 / FF Å] for vacancy creation, is then multiplied by the thickness of the U10Mo layer in the simulation (here: 15 µm) to achieve normalization per starting particle. The resulting unit for energy deposition is therefore [eV µm / FF Å] and [µm / FF Å] for vacancy creation.

To calculate the energy deposition and lattice damage of the Iodine-127 irradiation, an input set-up as shown in Fig. 1b has been used. The ion beam is represented by a point source, from which the particles were launched with 80MeV perpendicular to the surface of the sample with varying U8Mo or Al layer thickness.

3. Simulation results

The UMo and Al surface layer thicknesses significantly affect the energy deposition of the ions near and beyond the material interface. Figure 2 shows the relative effects of the heavy ions compared to the fission fragments for a 1 µm to 6 µm thick UMo layer on top, i. e. the effect the ions divided by the effects of the fission fragment. Figure 3 is the equivalent graph for the Al/U10Mo system. This relative effect ξ therefore has a unit of [1/µm] as the fission fragment effects were normalized by multiplication with the simulated volume. As effects were calculated per particle, ξ figuratively represents the "*number of fission fragments that yield the same effect as one ion"*.

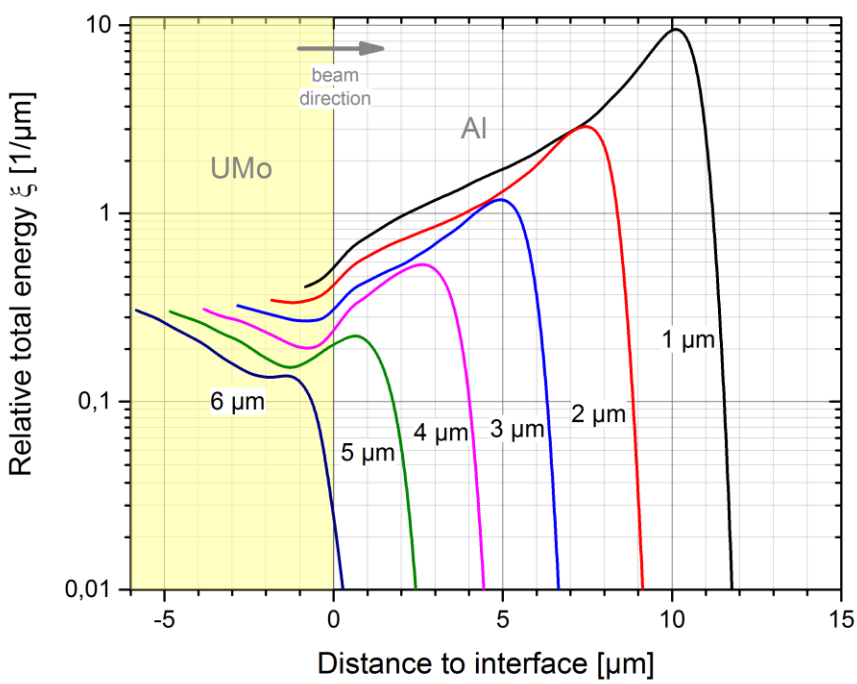

Figure 2: Relative total energy deposition for UMo layers ranging from 1µm to 6µm on top of an Aluminum substrate

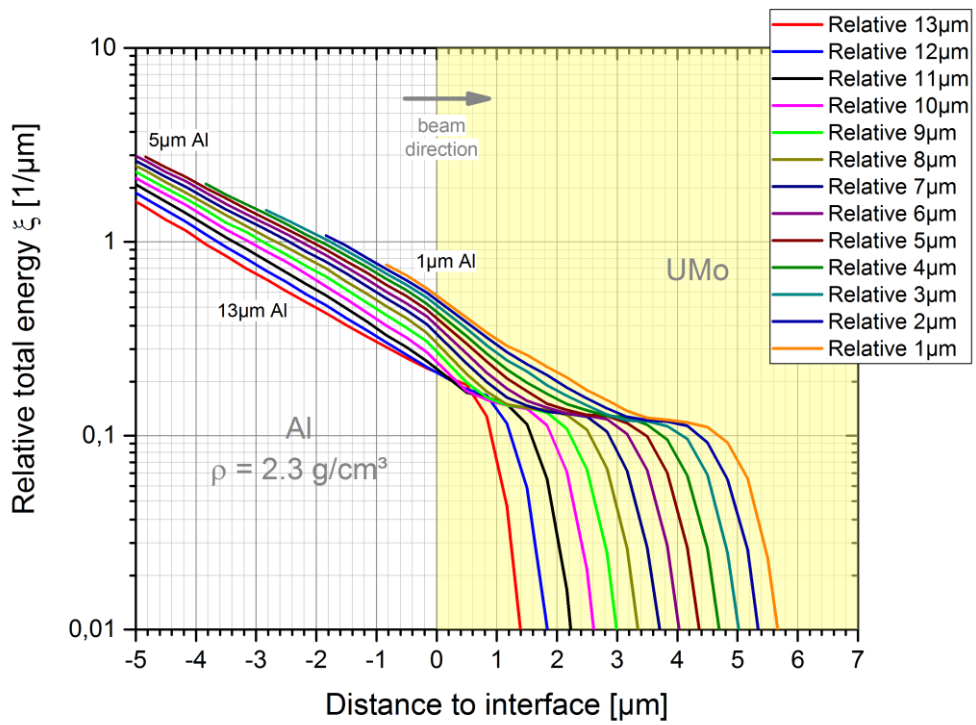

Figure 3: Relative total energy deposition for an Aluminium layer ranging from 1µm to 13µm on top of a UMo substrate.

In the following, it will be assumed that specifically the interface between Uranium and Aluminium is the point of interest, as this is the location where the IDL will develop during irradiation.

4. Equivalent radiation effects

4.1 Fission density

Given an in-pile test burn-up of n fissions per cm³ in a $d_{\text{fiss}}^{\text{irr}}$ thick layer, $N \propto 2n\, d_{\text{fiss}}^{\text{irr}}$ fission products would have started in the burnt Uranium volume; or $N \propto 2n\, d_{\text{fiss}}^{\text{sim}}$ fragments in a volume that would have had the same dimension as the simulated one. As simulations are normalized to 1 starting particle, the simulated fission fragment fluency must be scaled by a factor of $2n$ to match the real number of fission fragments.

For heavy ion irradiation, the simulated ion fluency must be scaled with the real ion fluency $\Phi = \int_0^{t_{\text{ion}}} \phi(t)dt = \phi t_{\text{ion}}$ assuming constant ion flux - over the irradiation time t_{ion}. Ideally, experimental and simulated fission density-dependent results X can therefore be scaled as

$$X_{\text{ion}}^{\text{irr}} = X_{\text{ion}}^{\text{sim}} \phi t_{\text{ion}}$$
$$X_{\text{fiss}}^{\text{irr}} = 2n X_{\text{fiss}}^{\text{sim}}$$

To be able to compare fission density-dependent effects from heavy ions and in-pile irradiation, obviously $X_{\text{ion}}^{\text{irr}} = X_{\text{fiss}}^{\text{irr}}$ must hold. The ratio $\xi = X_{\text{ion}}^{\text{sim}} / X_{\text{fiss}}^{\text{sim}}$ which appears in the resulting equations must be determined from the data resulting from the simulations. It depends on the heavy ion type, the ion energy and the thicknesses and materials of the layers of the sample used in the ion

irradiation experiment. The values for Iodine-127 at 80MeV on a U8Mo/Al-layer system can be obtained from Figure 4 specifically for the interface. The according values for an Al/U10Mo layer system are plotted in Figure 5. The final equations are therefore:

- To determine the heavy ion fluency Φ that is necessary to simulate a given burn-up n:

$$\Phi = 2n/\xi \tag{1}$$

- To determine the burn-up that corresponds to a given ion fluency:

$$n = \frac{1}{2}\Phi\xi \tag{2}$$

Applying this formalism to calculate in-pile equivalent burnups assumes that the geometry of the sample is not modified during irradiation (see sec. 4.3). Often, this is not the case as the fuel swells and interdiffusion layers form.

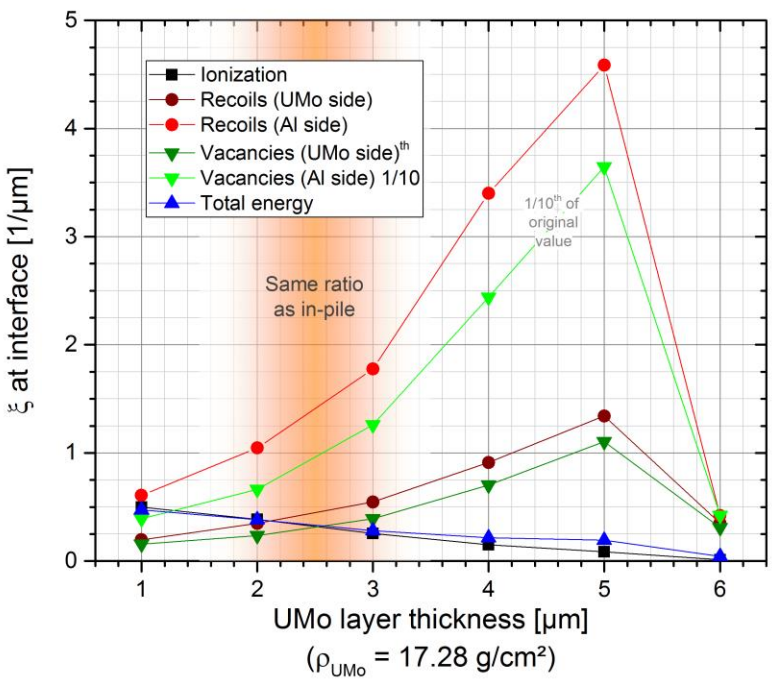

Figure 4: Relative energy deposition due to ionization, energy to recoils and vacancy creation of the fission fragments at the UMo/aluminum-interface for different UMo layer thicknesses. There is a sharp change of energy deposition to recoils and vacancy creation at the UMo/Al-interface, therefore these values are given twice, once for each side.

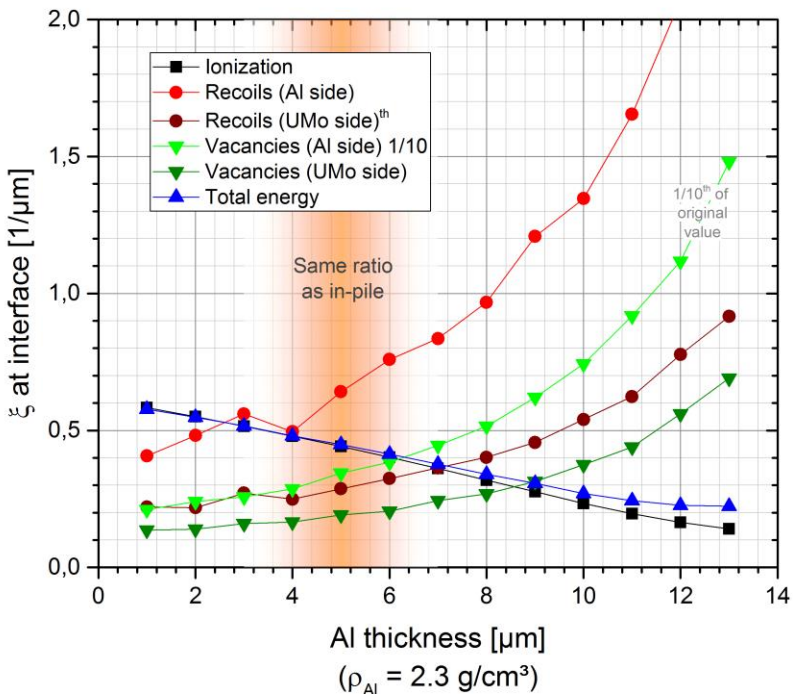

Figure 5: Relative energy deposition due to ionization, energy to recoils and vacancy creation of the fission fragments at the Al/UMo-interface for different Al layer thicknesses. There is a sharp change of energy deposition to recoils and vacancy creation at the Al/UMo-interface, therefore these values are given twice, once for each side.

4.2 Fission rate

Fission rate dependent effects can be compared in a similar way as fission density effects. Yet, fission rates usually vary notably during reactor operation, strongly decreasing with early poisoning of the fuel and then slower with increasing burn-up and depletion of fissionable material. Assuming an average fission rate $\dot{f}$ during early in-pile irradiation which is representative for the fission-rate dependent effect that should be studied and with constant heavy ion flux ϕ, the effects Y can again be compared:

$$Y_{\text{ion}}^{\text{irr}} = Y_{\text{ion}}^{\text{sim}}\phi$$
$$Y_{\text{fiss}}^{\text{irr}} = 2\dot{f}Y_{\text{fiss}}^{\text{sim}}$$

As $Y_{\text{ion}}^{\text{sim}} = X_{\text{ion}}^{\text{sim}}$ and $Y_{\text{fiss}}^{\text{sim}} = X_{\text{fiss}}^{\text{sim}}$ because no rate dependency was included in the simulations, we can again use the ratio $\xi = X_{\text{ion}}^{\text{sim}}/X_{\text{fiss}}^{\text{sim}}$ and obtain the following equations for conversion:

- To determine the heavy ion fluency that is necessary to simulate a given burn-up:

$$\phi = 2\dot{f}/\xi \tag{3}$$

- To determine the burn-up that corresponds to a given ion fluency:

$$\dot{f} = \frac{1}{2}\phi\xi \tag{4}$$

4.3 Limitations

The most notable restriction is that no time- and dose-dependent changes of the underlying material are considered. This particularly applies to the formation of diffusion zones in-between formerly

separated materials, e. g. the formation of UAlx-compounds between Uranium and Aluminium (see section 5). These layers, which can form rather early during irradiation, expose a different material composition and therefore different energy deposition / vacancy creation profiles. However, in many cases as long as these layers are thin, it is a reasonable approximation to use the value of ξ that was derived for the original, separated configuration: If the effects in-pile and by heavy ions are comparable, the change caused by the effect will affect both configurations in a very similar way. Therefore, ξ is not expected to change in such cases.

5. Interdiffusion layers

Jungwirth [8], based on Schilling [24] and Billington [23], has discussed that the irradiation enhanced diffusion which leads to the creation of this layer is mainly driven by thermal spiking, from ionization as well as recoils. Chiang [21] follows and extends this line of arguments. This is reasonable as the average ion energy is well above several 100 keV/u. Therefore, for the specific case of 127-I @ 80 MeV, ξ can be taken directly from the relative total energy deposition whenever the IDL formation itself is targeted.

Kim and Hofman [26] have developed a formula to predict the thickness d_{IDL} of interaction layer formation between UMo and Al during irradiation based on the data of several in-pile experiments:

$$d_{\mathrm{IDL}}^2 = A\dot{f}^p \exp\left[-\frac{q}{T}\right] t \cdot f_{\mathrm{Mo}} f_{\mathrm{Si}} \qquad (5)$$

In this equation, $A = 2.6 \cdot 10^{-8}\mu\mathrm{m}^2\mathrm{cm}^{3p}\mathrm{s}^{p\text{-}1}$ is the proportionality factor, $p = 0.5$ the power of the fission rate $\dot{f}$ that has been averaged over the irradiation time t and $q = 3850\mathrm{K}$ the fit parameter for the average irradiation temperature T (in the following entitled "normalization temperature"). f_{Mo} and f_{Si} are correction factors for the Molybdenum and Silicon content of fuel and matrix. No uncertainties were reported for the fitting constants, but an average deviation of 15% between measured and predicted IDL thickness can be estimated from the data provided by Kim [26]. Using eq. 4, the expected thickness of the IDL can be correlated with the ion flux.

5.1. The 4/16 ion irradiation campaign

An irradiation [25] using I-127 with an energy of 80 MeV on a total of 5 samples was carried out in April 2016 at the MLL accelerator [36] at TUM ("4/16 irradiation"). The approach was similar to former, qualitative irradiations [31, 8]. No beam wobbling was used. 4 samples were irradiated at a temperature of 413 K, 1 at 383 K. The samples consisted of a U10Mo substrate, PVD-coated with 13 µm aluminum (ρ = 2.3 g/cm³). Therefore, the Bragg peak was targeted directly on the Al/UMo interface ($\xi = 0.21\mu\mathrm{m}^{-1}$). Even though the ions reached the interface from the opposite direction, with the Bragg peak near the interface, there was no predominant direction for the ions due to the scattering in the Bragg peak.

In this campaign, fission density equivalents of up to $n = 5.8 \cdot 10^{20}\,\frac{\mathrm{fiss}}{\mathrm{cm}^3}$ were reached within 24 h. Exponential swelling caused by effects associated with the IDL in early in-pile experiments set in between $n = 1.5 - 2.0 \cdot 10^{21}\,\frac{\mathrm{fiss}}{\mathrm{cm}^3}$ [30], so these heavy ion irradiation results represent the early part of the IDL development (≈ 10% of maximum in-pile target burn-up).

The E-FUTURE and SELENIUM in-pile irradiations saw fission rates up to $\dot{f} = 8.9 \cdot 10^{14}\,\frac{\mathrm{fiss}}{\mathrm{cm}^3\,\mathrm{s}}$ during the first days of irradiation [7]. Previous experiments like IRIS-2 and FUTURE were

exposed to comparably lower fission rates ($\dot{f} = 2.8 \cdot 10^{14} \frac{\text{fiss}}{\text{cm}^3\,\text{s}}$ and $\dot{f} = 4.2 \cdot 10^{14} \frac{\text{fiss}}{\text{cm}^3\,\text{s}}$ respectively). Due to the varying intensity across the geometric beam profile, in the 4/16 ion campaign, an equivalent fission rate range from $\dot{f} \approx 10^{12} \frac{\text{fiss}}{\text{cm}^3\,\text{s}}$ up to $\dot{f} = 9.6 \cdot 10^{15} \frac{\text{fiss}}{\text{cm}^3\,\text{s}}$ was achieved in a single irradiation, i.e. the full range from below the lowest in-pile fission rate areas up to 17 times higher rates than in the high fission rate area of SELENIUM and E-FUTURE.

5.2. Geometric beam profile reconstruction

In the 4/16 ion experiment, the geometric flux distribution could not be measured directly. However, it was known from previous, elaborate measurements, that the beam profile was a 2D Gaussian:

$$\phi(x,y) = \frac{A}{\sigma_x \sigma_y} \cdot \exp\left[-\frac{1}{2}\left(\frac{x^2}{\sigma_x^2} + \frac{y^2}{\sigma_y^2}\right)\right] \tag{6}$$

To quantitatively evaluate the irradiation, the width and center intensity of this Gaussian profile had to be determined. The ion beam left a characteristic, elliptical footprint on the sample surface, whose dimensions could be determined using optical microscopy (Figure 6).

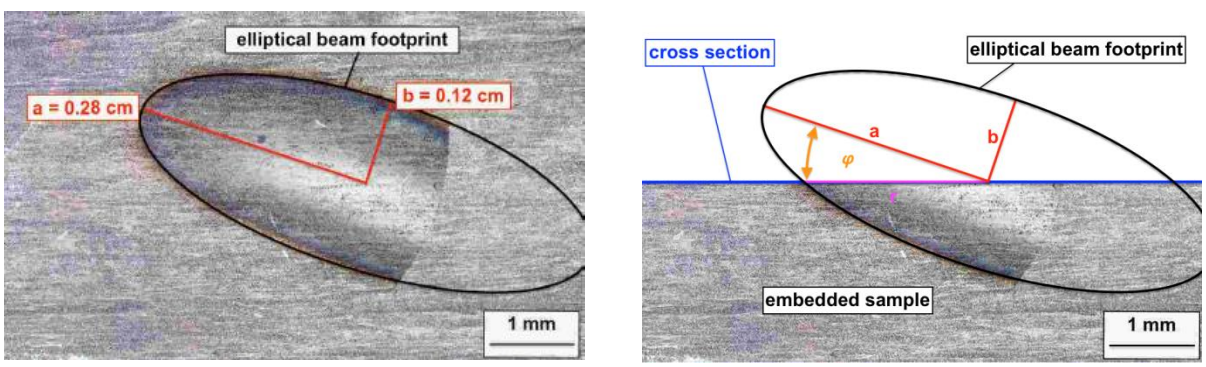

Figure 6: Footprint of the ion beam on the Al sample surface with dimensions as determined by optical microscopy. The sharp edge in the right part of the ellipse originates from an aperture that was used to fix the sample in the beam.

Once the axes a and b were determined, the sample was cut, embedded into resin, and polished to obtain a cross section through the beam center (Figure 6 right side, Figure 7). Any straight cut through a 2D Gaussian is again a Gaussian, therefore the width of the resulting 1D Gaussian can be determined from:

- the distance r_{border} between the center and the border of the footprint along the cutline,
- the angle φ between the major axis a and the cutline and
- the fluxes at beam center $\phi_{\text{max}} = \phi(0,0)$ and at the border of the footprint, ϕ_{border}.

r_{border} was obtained from geometric measurements of the sample, then the angle φ can be calculated from elliptic coordinates[1] or vice versa. The value was verified by direct measurements along the cut-line of the sample. The latter two values cannot be accessed directly but need to be obtained from the resulting IDL, i.e. calculated indirectly. Therefore, SEM pictures were taken along the cutline and the thickness of the IDL was measured at three equidistant points per image.

[1] $r_{\text{border}} = \frac{ab}{\sqrt{b^2 \cos\varphi + a^2 \sin\varphi}}$

One image was taken every 10 µm.

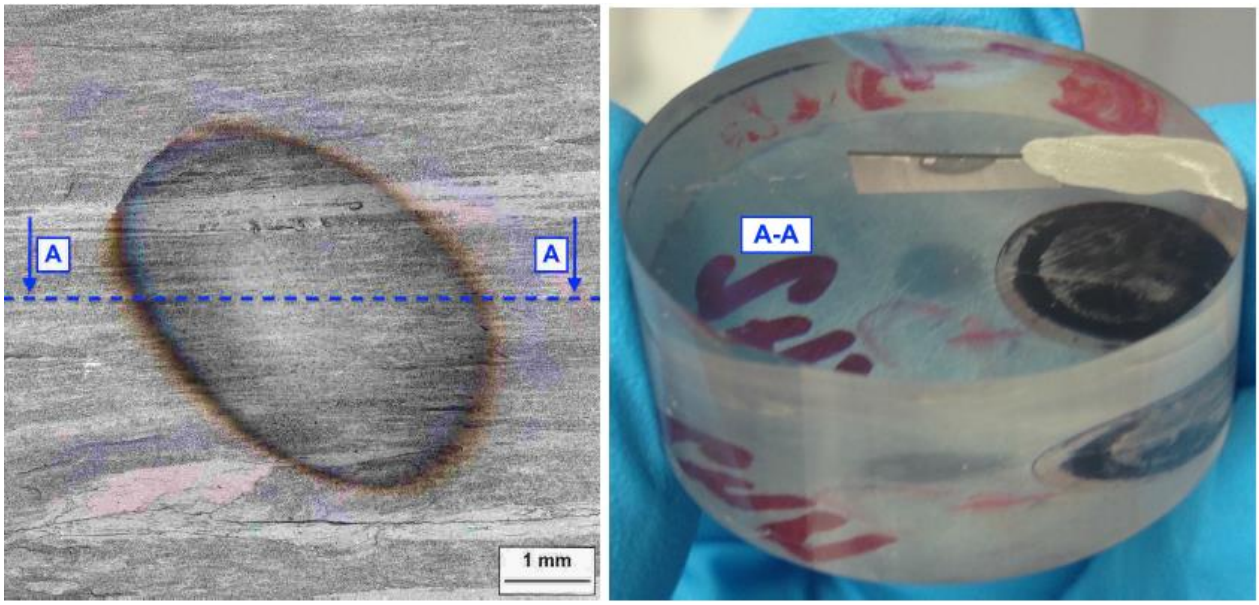

Figure 7: Sample preparation for PIE: Definition of a cut-line, and polished sample embedded into the transparent resin.

In a first step, it needs to be assumed that the relation $d_{\mathrm{IDL}} \propto \phi^{1/4}$ in eq. (5), is true. This assumption is necessary for the relative flux profile reconstruction, not for absolute flux values. However, employing this assumption means that the absolute value of p cannot be verified in a later analysis based on this reconstruction, as this would result in a circular statement. Nevertheless, trends of p can still be studied. The absolute values of the ion flux profile are obtained from the total ion flux, i.e. the spatially integrated ϕ. This value can be calculated from the current I which was measured using Faraday cups in the experimental beam setup. This way, the center flux

$$\phi_{\max} = \frac{4}{ab}\frac{I}{\pi L q_e}\ln\left[\frac{d_{\mathrm{IDL}}^{\max}}{d_{\mathrm{IDL}}^{\mathrm{border}}}\right]$$

is obtained, where L is the charge state of the ion (4/16: 7+) and q_e the elementary electric charge. The thicknesses $d_{\mathrm{IDL}}^{\max}$ and $d_{\mathrm{IDL}}^{\mathrm{border}}$ are either measured directly or obtained from fits on the ion flux profile. The widths of the 2D Gaussian can then be calculated by

$$\sigma_x = a\sqrt{8 \cdot \ln\left[\frac{d_{\mathrm{IDL}}^{\max}}{d_{\mathrm{IDL}}^{\mathrm{border}}}\right]}$$

and similarly for σ_y. The width w of the 1D Gaussian along the cutline is finally determined from σ_x, σ_y and φ.

$$w = \frac{\sigma_x \sigma_y}{\sqrt{\sigma_y^2 \cos\varphi + \sigma_x^2 \sin\varphi}}$$

In the last step, the flux along the cutline is calculated using

$$\phi(r) = \frac{4}{ab}\frac{I}{\pi L q_e}\ln\left[\frac{d_{\mathrm{IDL}}^{\max}}{d_{\mathrm{IDL}}^{\mathrm{border}}}\right]\exp\left[-\frac{1}{2}\frac{r^2}{w^2}\right].$$

This way, the geometric flux profile of the ion beam has been reconstructed, utilizing only $p = 0.5$ from eq. (5). Figure 8 shows a reconstructed beam profile, obtained from fitting on the measured data points.

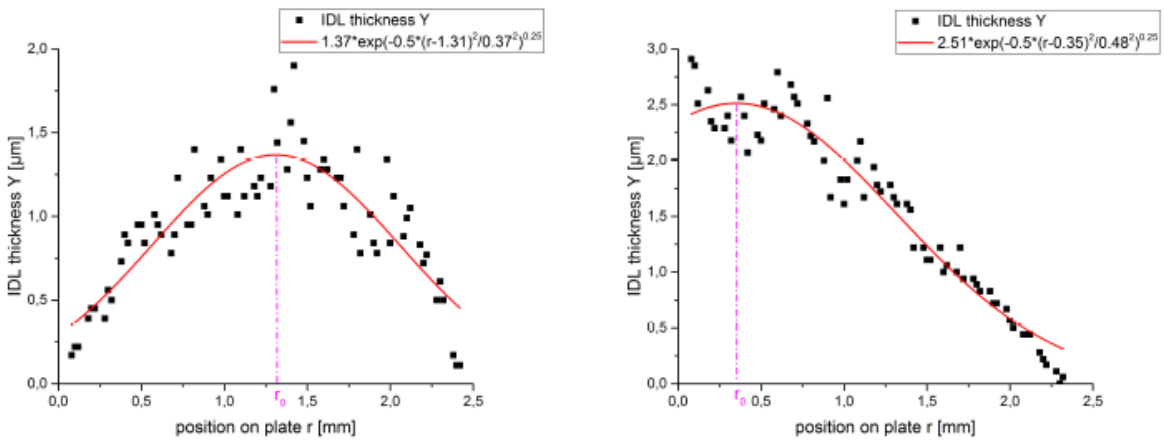

(a) Sample 1 (b) Sample 2

Figure 8: Two of the five irradiated samples, with measured IDL thickness and a fit based on the $d_{\mathrm{IDL}} \propto \phi^{1/4}$ proportionality

5.3. Quantitative evaluation of IDL development

The results from the 4/16 ion irradiation allow for a first verification of the flux - fission rate conversion. Figure 9 shows the deviation between the IDL thickness calculated according to equations 4 and 5 and the actual measured values: Even though significant scattering is present, which is attributed to the general fluctuation of IDL thicknesses that is also observed in-pile and to suboptimal sample quality, prediction and measurement match well within the uncertainties of the experiment and the assumed uncertainties of eq. 5.

The ion irradiations cover a large variety of fission rate and burn-up equivalents. Eq. 5 can be solved for the proportionality factor A, with the values of d_{IDL} and T taken from measurements and $\dot{f}$ from the reconstructed flux profile, calculated using eq. 4 with $p = 0.5$. A plot of A over the equivalent fission density $n = \dot{f}t$ is shown in Figure 10. The average value of $A = 2.86 \cdot 10^{-8} \pm 0.10 \cdot 10^{-8}$ from ion irradiations matches very well with the one found by Kim and Hofman [26] for in-pile experiments ($A = 2.6 \cdot 10^{-8}$).

As the samples were irradiated at two different temperatures (383K and 413K) and for different time spans (5 h to 27.85 h), the experiment furthermore confirms the proportionality $d_{\mathrm{IDL}} \propto \sqrt{t}$ and, to a lesser extent, the temperature dependence.

The sheer proportionality between IDL thickness and ion flux for a single irradiation is independent from the value of ξ in eq. 4. As the proportionality was verified over a large range of fission densities, the correct absolute value of A which was derived from ion experiment therefore confirms eq. 4 and the calculated absolute value of ξ.

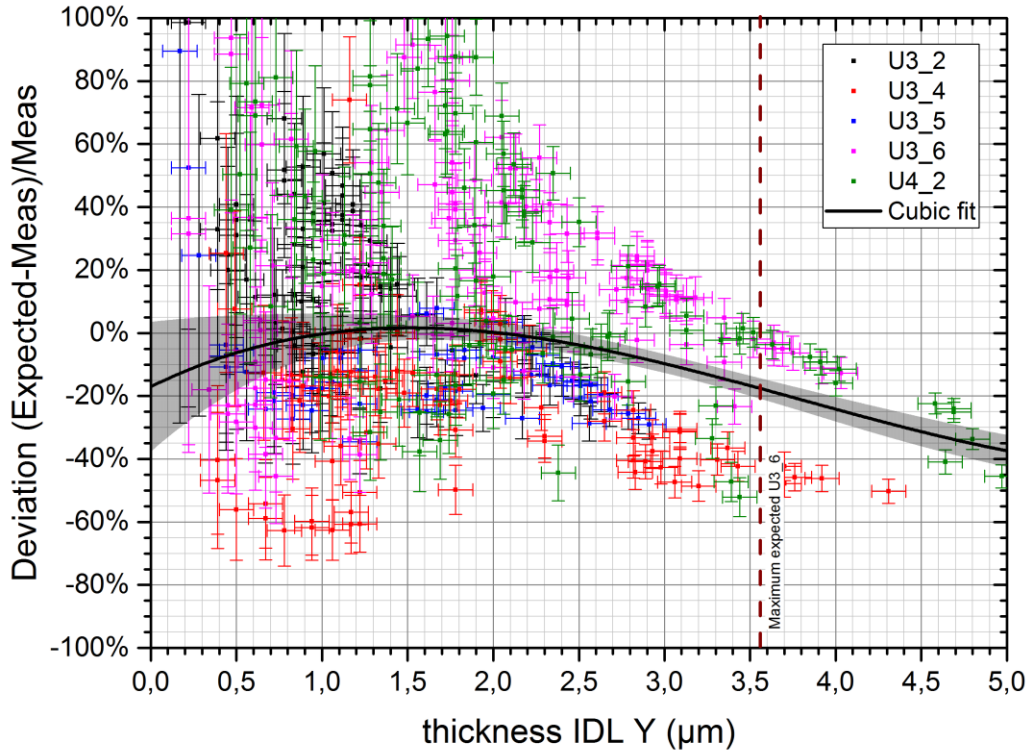

Figure 9: Deviation of the IDL thickness measured by Hingerl [30] compared to the value expected according to the conversion presented in this work and the formula 5 by Kim [31], i.e. y-axis is difference between expected and measured value, divided by measured value. Hingerl irradiated five samples at 413K and one at 383K (U3_5), the maximum IDL thickness being expected for sample U3_6. The use of a cubic fit is arbitrary to visualize a trend.

As last item, the data from the 4/16 campaign can be used to analyze the fission rate exponent p for potential trends. The absolute value of the exponent cannot be determined as $p = 0.5$ was already used in the reconstruction of the flux profile. The result is depicted in Figure 11. Here, eq. 5 has been solved for p and data taken as described above for the proportionality factor $A = 2.6 \cdot 10^{-8}$.

One of several possible explanations for the observation of an increased swelling at high burn-ups in the SELENIUM and E-FUTURE irradiation is the assumption of an accelerated IDL growth at fission rates $\dot{f} \gtrsim 7 \cdot 10^{14} \frac{\text{fiss}}{\text{cm}^3\,\text{s}}$. However, if p would somehow depend on the fission rate $\dot{f}$, this would be visible in form of a trend in Figure 11. Yet, no trend is visible.

It should be noted that A and p are not completely independent but correlated to some extent. This means that both conclusions partially rely on each other. For the special case of the fission rate-dependency discussed above, a fission rate dependence of A could also be found in p (Figure 10) and vice versa. Yet, as A as well as p confirm the ion flux-fission rate conversion and eq. 5, this partial correlation does not influence the findings.

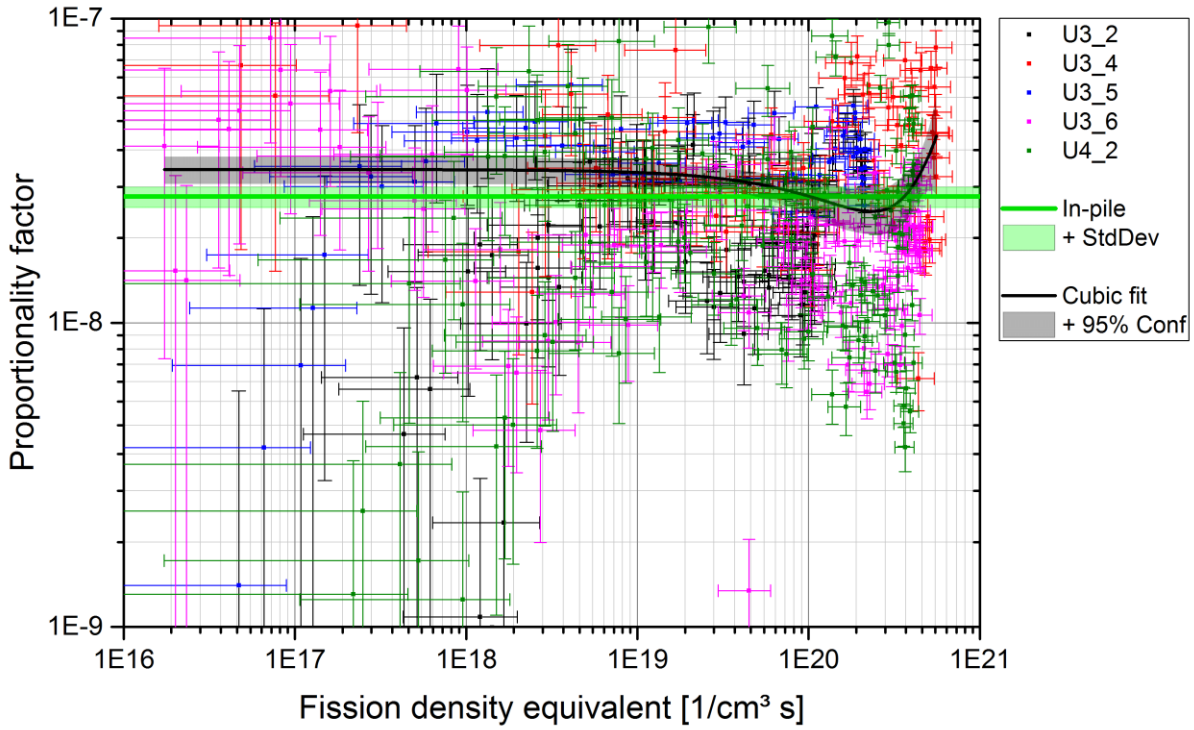

Figure 10: Measured proportionality factor A from eq. 5. The uncertainty of the in-pile constant $A = 2.6 \cdot 10^{-8}$ was estimated from the total uncertainty of eq. 5. The average value for the ion experiments of Hingerl [30] is $A = 2.86 \cdot 10^{-8} \pm 0.10 \cdot 10^{-8}$

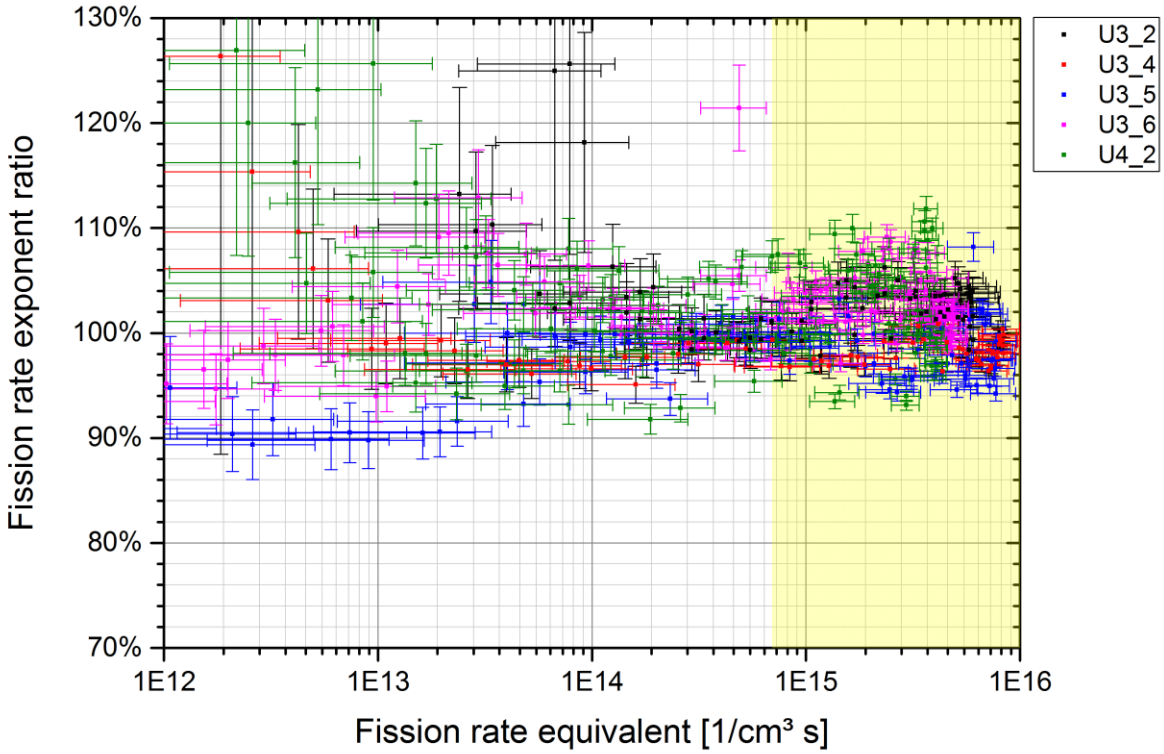

Figure 11: Trend analysis for the exponent p in eq. 5. An increased swelling rate has been observed in in-pile tests where the maximum fission rate $\dot{f}$ was above $7 \cdot 10^{14} \frac{\text{fiss}}{\text{cm}^3\,\text{s}}$ (yellow area). This increase does not seem to be connected to pure IDL growth.

Zweifel and Chiang [32, 21] conducted numerous ion beam experiments between 2011 and 2015 but used a wobbled[2] ion beam and therefore could report only area averaged fluxes. Thereby, eq. 5 is not fully applicable as the actual real fission rate equivalent cannot be calculated. Consequently, the IDL thicknesses reported in these works are considerably thinner than what would be expected from eq. 5. However, it should be possible to test the temperature-dependency of the Arrhenius equation with the data obtained in these experiments. Figure 12 shows a temperature dependent fit of the Arrhenius term using $q = 3850\text{K}$ (solid line) on the data from these irradiations. While the trend is obvious, the results of the orthogonal distance regression fit with q as free parameter suggest a considerably higher value of $q = 8820\text{K} \pm 1763\text{K}$ (dashed line). Earlier iterations of Kim's equation [33, 34, 35] utilized q-values up to 9141K, especially for low irradiation temperatures < 393K, which would agree with Zweifel's data. The reason for the deviation is currently unknown but might also be connected to the use of a wobbled beam. Furthermore, q and A are highly correlated in these fits.

[2] "Wobbling" means that the beam is periodically moved independently in x- and y-direction, typically with a few Hz and different frequencies and amplitudes for the two directions. This way, a "beam pattern" is drawn on the sample, which covers the whole sample almost homogeneously if the wobbling parameters have been chosen carefully. The beam pattern is therefore the convolution of the 2D Gaussian and the periodic movement function.

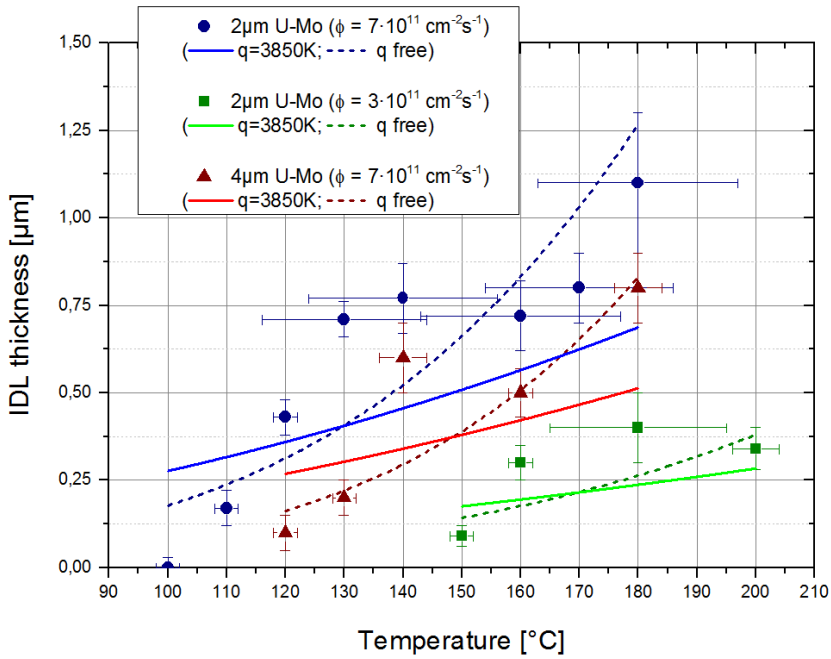

Figure 12: IDL thicknesses as measured by Zweifel [40] and two orthogonal regression fits of the temperature dependency of the Arrhenius equation 5 for each data set, one with q = 3850K (solid line) and one with q as free fit parameter (dashed line). q was evaluated to 8310K ± 2613K, 7898K ± 4770K and 9698K ± 2761K respectively, yielding a weighted average of $q = 8820\text{K} \pm 1763\text{K}$. Reported fluxes are area-averaged as the ion beam was wobbled.

6. Summary

Fission rate and fission density equivalents are proportional to the flux and fluency of heavy ions if the right kind of ion is employed. The proportionality factor ξ depends on ion type, energy and the material layer system that is used to simulate an in-pile irradiation by out-of-pile means. The factor ξ can be obtained from SRIM/TRIM calculations.

An interdiffusion layer develops during irradiation at the interface between UMo and Al if no protective measures like silicon addition to the matrix or coating of the particles are taken. Kim and Hofman [26] have derived a formula (eq. 5) from in-pile data for prediction of the IDL thickness based on fission rate, irradiation time and temperature. The formula is in very good agreement with heavy ion irradiation data from the 4/16 experiment when ion fluxes and fluencies are converted to fission rate and burn-up equivalents using the approach presented in eq. 4 and 2.

It was shown that the proportionality constant A in eq. 5 is independent of the fission density, i. e. that the IDL develops according to $d_{\text{IDL}} \propto \sqrt{t}$. It was furthermore shown that the exponent p of the fission rate does not depend on the fission rate but is constant, too. However, it was not possible to verify the absolute value $p = 0.5$ as this value was used to reconstruct the ion flux profile. The data of 4/16 is also in agreement with the temperature dependence and $q = 3850\text{K}$, however only one sample was irradiated at 383K, all others at 413K. The more extensive data set of Zweifel [32] suggests a considerably higher value of $q = 8820\text{K} \pm 1763\text{K}$, which however does not seem to agree with the current data from 4/16 but with earlier iterations of Kim's formula. It remains unclear at this time how the beam-wobbling used by Zweifel affects the IDL growth and thereby

the conversion algorithm.

Once it is fully understood how to quantitatively interpret the data from heavy ion irradiations and how to compare it to in-pile data, this tools will be able to even more reliably, quicker and easier answer specific questions in nuclear fuel development. This paper presented a first attempt for the quantitative evaluation of ion beam experiments as well as of the conversion of ion effects to their in-pile equivalents. The IDL growth dynamics were verified successfully.

7. Acknowledgements

The authors would like to thank the MLL staff for their great support during our beam-times and also in the times in-between. Your knowledge and input is always appreciated. A huge “Thank you” also goes out to everybody participating in the beam time shifts: Christian Reiter, Tanja Huber, Bruno Baumeister and Christian Schwarz.

The support of Ann Leenaers (SCK•CEN), Gerard Hofman and Yeon Soo Kim (Argonne National Laboratory) in terms of data and discussion of the results is greatly appreciated.

The work on the flux – fission density conversion was supported by a combined grant (FRM1318) from the Bundesministerium für Bildung und Forschung (BMBF) and the Bayerisches Staatsministerium für Bildung und Kultus, Wissenschaft und Kunst (StMBW).

The work on the ion beam irradiation was supported by the European Commission in the framework of HORIZON 2020 through Grant Agreement 661935 in the HERACLES CP project.

8. References

[1] M. Meyer, G. Hofman, S. Hayes, C. Clark, T. Wiencek, J. Snelgrove, R. Strain, K.-H. Kim, Low-temperature irradiation behavior of uranium-molybdenum alloy dispersion fuel, Journal of Nuclear Materials 304 (2002) 221–236.

[2] S. van den Berghe, W. van Renterghem, A. Leenaers, Transmission electron microscopy investigation of irradiated U7wt%Mo dispersion fuel, Journal of Nuclear Materials 375 (2008) 340–346.

[3] A. Leenaers, S. van den Berghe, E. Koonen, C. Jarousse, F. Huet, M. Trotabas, M. Boyard, S. Guillot, L. Sannen, M. Verwerft, Post-irradiation examination of uranium-7 wt% molybdenum atomized dispersion fuel, Journal of Nuclear Materials 335 (2004) 39–47.

[4] G. Hofman, M. Finlay, Y. Kim, Post irradiation analysis of low enriched U-Mo/Al dispersion fuel miniplate tests, RERTR 4&5, in: Proceedings of the 26. International Meeting on Reduced Enrichment for Research and Test Reactors (RERTR), 2004.

[5] P. Lemoine, D. Wachs, High density fuel development for Research Reactors, in: Proceedings of the International Conference on Research Reactors: Safe Management and Effective Utilization, IAEA, Sydney, 2007, IAEA-CN-156.

[6] Y. Kim, G. Hofman, Irradiation behavior of the interaction product of UMo fuel particle dispersion in an Al matrix, Journal of Nuclear Materials 425 (2011) 181–187.

[7] S. van den Berghe, Y. Parthoens, F. Charollais, Y. Kim, A. Leenaers, E. Koonen, V. Kuzminov, P. Lemoine, C. Jarousse, H. Guyon, D. Wachs, D. Keiser, A. Robinson, J. Stevens, G. Hofman, Swelling of U(Mo)-Al8Si) dispersion fuel under irradiation – Non-destructive analyses of the LEONIDAS E-FUTURE plates, Journal of Nuclear Materials 430 (2012) 246–258.

[8] R. Jungwirth, Irradiation behavior of modified high-performance nuclear fuels, Ph.D. thesis, Technische Universität München (2011).

[9] A. Izhutov, et al., The status of LEU U-Mo fuel investigation in the MIR reactor, in: Proceedings of the 31th International Meeting on Reduced Enrichment for Research and Test Reactors (RERTR), Bejing, 2009.

[10] S. van den Berghe, A. Leenaers, C. Detavernier, SELENIUM fuel: Surface engineering of U(Mo) particles to optimise fuel performance, in: Proceedings of the International Topical Meeting on Research Reactor Fuel Management (RRFM), Marrakesh, 2010.

[11] R. Jungwirth, T. Zweifel, H.-Y. Chiang, W. Petry, S. van den Berghe, A. Leenaers, Heavy ion irradiation of UMo/Al samples PVD coated with Si and ZrN layers, Journal of Nuclear Materials 434 (2013) 296–302.

[12] P. Lemoine, Status of the french CEA program for the development and the qualification of high density fuel for the JHR project, in: Proceedings of RERTR 2005, Boston, USA, 2005.

[13] M. Ripert, S. Dubois, P. Boulcourt, S. Naury, P. Lemoine, IRIS3 experiment Status and result of thickness increase, in: Proceedings of the 10th International Topical Meeting on Research Reactor Fuel Management (RRFM), Sofia, 2006.

[14] G. Hofman, Y. Kim, H. Ryu, J. Rest, D. Wachs, M. Finlay, Attempt to solve the instability in the irradiation behavior of low enriched UMo/Al dispersion fuel, in: Proceedings of RRFM 2006, Sofia, Bulgaria, 2006.

[15] Y. Kim, G. Hofman, A. Robinson, Effect of Si addition in Al in UMo /Al dispersion plates: Observations from side-by-side irradiations from RERTR-6, -7a, -9a and -9b, in: Proceedings of RRFM 2009, Vienna, Austria, 2009.

[16] N.Wieschalla, A. Bergmaier, P. B¨oni, K. B¨oning, G. Dollinger, R. Grossmann, W. Petry, A. Röhrmoser, J. Schneider, Heavy ion irradiation of UMo-Al dispersion fuel, Journal of nuclear materials 357 (2006) 191–197.

[17] H. Palancher, N. Wieschalla, P. Martin, R. Tucoulou, C. Sabathier, W. Petry, J. Berar, C. Valot, S. Dubois, Uranium-Molybdenum nuclear fuel plates behavior under heavy ion irradiation an X-ray diffraction analysis, Journal of Nuclear Materials 385 (2009) 449–455.

[18] R. Hengstler, L. Beck, H. Breitkreutz, C. Jarousse, R. Jungwirth,W. Petry, W. Schmid, J. Schneider, N. Wieschalla, Physical Properties of Monolithic U8wt.-%Mo, Journal of Nuclear Materials 402 (2010) 74–80.

[19] H.-Y. Chiang, T. Zweifel, H. Palancher, A. Bonnin, L. Beck, P. Weiser, M. Döblinger, C. Sabathier, W. P. R. Jungwirth, Evidence of amorphous interdiffusion layer in heavy ion irradiated U-8wt%Mo/Al interfaces, Journal of Nuclear Materials 440 (2013) 117–123.

[20] E. Welcomme, H. Palancher, C. Sabathier, P. Matin, J. Allenou, C. Valot, F. Charollais, M. Anselmet, R. Jungwirth, W. Petry, L. Beck, C. Jarousse, P. Lemoine, Heavy ion irradiation of UMo7/Al fuel: methodological approach, in: Proceedings of the International Topical Meeting on Research Reactor Fuel Management (RRFM), Vienna, 2009.

[21] H.-Y. Chiang, Material selection of UMo fuel for research reactors: Swift heavy ion irradiation studies, Ph.D. thesis, Technische Universität München (2014).

[22] T. Zweifel, N. Valle, C. Grygiel, I. Monnet, L. Beck,W. Petry, Kr implantation into heavy ion irradiated monolithic u-mo/al systems: Sims and SEM investigations, Journal of Nuclear Materials 470 (2016) 251–257.

[23] D. Billington, J. Crawford, Radiation damage in solids, Princeton University Press, New Jersey, 1961.

[24] W. Schilling, H. Ullmaier, Physics of radiation damage, in: B. Frost (Ed.), Material Science and Technology Volume 10B, Nuclear Materials, 1st Edition, VCH Verlagsgesellschaft mbH, Weinheim, Deutschland, 1994.

[25] J. Hingerl, Evolution of the inter diffusion layer of UMo/Al nuclear fuels during heavy ion irradiation, Bachelorthesis (7/2016).

[26] Y. Kim, G. Hofman, H. Ryu, J. Park, A. Robinson, D. Wachs, Modeling of interaction layer growth between U-Mo particles and an Al matrix, Nuclear Engineering and Technology 45 (2013) 827–837.

[27] J. Ziegler, SRIM, http://www.srim.org (2010).

[28] J. Ziegler, J. Biersack, M. Ziegler, SRIM - The stopping and range of ions in matter, SRIM Co., Chester - USA, 2008

[29] A. Heldmann, Energie- und Gitterschädenverteilung am Übergang UMo-Al: Vergleich von Spaltprodukten und Schwerionen, Bachelorthesis (8 2012).

[30] P. Lemoine, J. Snelgrove, N. Arkhangelsky, L. Alvarez, UMo dispersion fuel results and status of qualification programs, in: Proceedings of the 8th International Topical Meeting on Research Reactor Fuel Management (RRFM), Munich, 2004.

[31] N. Wieschalla, Heavy ion irradiation of UMo/Al dispersion fuel, Dissertation, TUM (2006).

[32] T. Zweifel, Fission gas behaviour and interdiffusion layer growth in inpile and out-of-pile irradiated u-mo/al nuclear fuels, Ph.D. thesis, Technische Universität München (2014).

[33] Y. Kim, G. Hofman, H. Ryu, Irradiation-enhanced interdiffusion in the diffusion zone of u-mo dispersion fuel in al, Journal of Phase Equilibria and Diffusion 27 (2006) 614–621.

[34] D.Wachs, D. Burkes, S. Hayes,W. Skerjanc, G. Hofman, Y. Kim, H. Ryu, Modeling the integrated performance of dispersion and monolithic u-mo based fuels, in: Proceedings of the International Meeting on Reduced Enrichment for Research and Test Reactors (RERTR), Cape Town, South Africa, 2006.

[35] Y. Kim, G. Hofman, P. Medvedev, G. Shevlyakov, A. Robinson, H. Ryu, Post irradiation

analysis and performance modeling of dispersion and monolithic u-mo fuels, in: Proceedings of the International Meeting on Reduced Enrichment for Research and Test Reactors (RERTR), Prague, Czech Republic, 2007.

[36] http://www.bl.physik.uni-muenchen.de/

[37] A. Leenaers, S. van den Berghe, W, van Renterghem, F. Charollais, P. Lemoine, C. Jarousse, A. Röhrmoser, W. Petry, Irradiation behaviour of ground U(Mo) fuel with and without Si added to the matrix, Journal of Nuclear Materials 412 (2011) 41-52